Analytical Performance Evaluation of Various Frequency Reuse and Scheduling Schemes in Cellular OFDMA Networks

Masood Maqbool, Philippe Godlewski, Marceau Coupechoux, Jean-Marc Kélif

Analytical Performance Evaluation of Various Frequency Reuse and Scheduling Schemes in Cellular OFDMA Networks

Masood Maqbool

TELECOM ParisTech & CNRS LTCI, 46 rue Barrault, 75013 Paris, France

Philippe Godlewski

TELECOM ParisTech & CNRS LTCI, 46 rue Barrault, 75013 Paris, France

Marceau Coupechoux

TELECOM ParisTech & CNRS LTCI, 46 rue Barrault, 75013 Paris, France

Jean-Marc Kélif

France Telecom R&D, Issy-les-Moulineaux, France

Abstract

In this paper, we present an analytical solution to carry out performance analysis of various frequency reuse schemes in an OFDMA based cellular network. We study the performance in downlink in terms of signal to interference (SIR) ratio and total cell data rate. The latter is analyzed keeping in view three different scheduling schemes: equal data rate, equal bandwidth and opportunist. Analytical models are proposed for integer frequency reuse (IFR), fractional frequency reuse (FFR) and two level power control (TLPC) schemes. These models are based on a fluid model originally proposed for CDMA networks. The modeling key of this approach is to consider the discrete base stations entities as a continuum. To validate our approach, Monte Carlo simulations are carried out. Validation study show that results obtained through our analytical method are in conformity with those obtained through simulations. We present a comparison between above three frequency reuse schemes and three scheduling schemes. We also propose an optimal tuning of involved parameters (inner cell radius and power ratios).

Key words: OFDMA, Fluid Model, SINR, Frequency Reuse, IFR, FFR, Scheduling, Equal data rate scheduling, Equal bandwidth scheduling, Opportunist
PACS:

1 Introduction

Orthogonal frequency division multiple access (OFDMA) is a promising multiple access technique being proposed for next generation mobile networks. The underlying technology for OFDMA based systems is orthogonal frequency division multiplexing (OFDM). With OFDM, available spectrum is split into a number of parallel orthogonal narrowband subcarriers. These subcarriers can be independently assigned to different users in a cell. Resources of an OFDMA system occupy place both in time (OFDM symbols) and frequency (subcarriers) domains thus introducing both the time and frequency multiple access [7].

Co-channel interference (CCI) limits the spectral efficiency of an integer frequency reuse 1 (IFR1) cellular network (cf. section 3 for an introduction on IFR). The CCI becomes more critical for the users present in the border area of a cell. To combat this problem in an OFDMA based system, fractional frequency reuse (FFR) has been proposed in [1]. In FFR, cell is divided into inner (close to base station) and outer (border area) regions. Available bandwidth is divided among inner and outer regions in a way that former employs reuse 1 while the latter applies frequency reuse 3. Hence, users located in cell border mitigate CCI because of frequency reuse 3. By properly adjusting the sizes of inner and outer regions, spectral efficiency can be improved.

Authors of [8] studied the performance of FFR for 3GPP/ 3GPP2 OFDMA systems and call it soft frequency reuse. Authors have used system level simulations (SLS) in their analysis. In [10] and [9], author has studied the FFR in a IEEE 802.16 based system. Author has proposed an interference coordination system, which focuses on the scheduling of users. Proposed algorithm is implemented in SLS to present results. Two new algorithms, fractional time reuse (FTR) and fractional time and frequency reuse (FTFR), are proposed in [2] to cater for reduced capacity in the border area of cell because of FFR. In [13], authors have studied the capacity of a WiMAX system in presence of FFR. In [3] also, performance of a FFR system is analyzed through simulations.

In contrast to existing work, in this paper we present approximate analytical models for IFR and FFR schemes of an OFDMA based cellular network. We derive expressions to calculate SIR at a given distance from base station (BS) and compute spectral efficiency using Shannon's classical formula. We also determine total cell data rate considering three different scheduling schemes: equal data rate, equal bandwidth and opportunist.

Email addresses: masood.maqbool@telecom-paristech.fr (Masood Maqbool), philippe.godlewski@telecom-paristech.fr (Philippe Godlewski), marceau.coupechoux@telecom-paristech.fr (Marceau Coupechoux), jeanmarc.kelif@orange-ftgroup.fr (Jean-Marc Kélif).

This paper extends the framework, based on a fluid model, proposed in [4] and [5]. The model provides a simple closed-form formula for the other-cell interference factor f on the downlink of CDMA networks as a function of the distance to the BS, the path-loss exponent, the distance between two BS, and the network size. The modeling key of this approach is to consider the discrete BS entities of a cellular network as a continuum.

Rest of the paper is organized as follows: section 2 introduces notations used throughout the paper and recalls the main result of the fluid model. Section 3 focuses on IFR and derives SIR and spectral efficiency expressions for both reuse 1 and reuse K. The case of FFR is studied in section 4. A two level power control scheme used in conjunction with FFR is considered in section 5. In section 6, three frequency reuse schemes (IFR, FFR and TLPC) are compared in terms of SINR and total cell data rate. Finally, section 7 discusses the conclusion of this analysis.

2 Fluid Model and Notations

In this section, we explain the application of fluid model to an OFDMA system. We focus on the downlink and consider a single subcarrier. BS have omni-directional antennas, such that one BS covers a single cell. If a user u is attached to a station b (or serving BS), we write $b = \psi(u)$.

The propagation path gain $g_{b,u}$ designates the inverse of the pathloss pl between station b and user u, $g_{b,u} = 1/pl_{b,u}$. In the rest of this paper, we assume that $g_{b,u} = Ar_{b,u}^{-\eta}$, where A is a constant, $r_{b,u}$ is the distance between BS b and user u and η (> 2) is the path-loss exponent.

Before presenting the expression of fluid model, we establish the following terms:

- P_{Tx} is the transmitted power per subcarrier. We assume that the output power per subcarrier is constant. Only in section 5, we consider two possible values of output power per subcarrier: P_i for the inner region of the cell and P_o for the outer region. In this paper, we do not consider dynamic power allocation per subcarrier since in current OFDMA systems (WiMAX, Long Term Evolution), output power per subcarrier is constant;
- $S_{b,u} = P_{Tx}\, g_{b,u}$ is the useful power received at user u from station b (for traffic data);
- W is the total system bandwidth and W_u is the bandwidth dedicated to user u;
- R, R_c and R_{nw} are respectively the cell radius, half distance between base stations and network range (see Fig. 1);

- R_e is the radius of a circular region whose area is equal to that of the hexagon with length of each side equal to R. Based on definitions of R_e, R and R_c, it can be deduced that $R_e = aR_c = a\frac{\sqrt{3}}{2}R$, where $a = \sqrt{\frac{2\sqrt{3}}{\pi}}$.
- ρ_u, ρ_{BS} and N_u are respectively the user density, BS density and number of users per cell;
- D_u is the data rate allocated to a user and D_T is the total cell data rate;
- N_{BS} represents the total number of base stations in the network.

The total amount of power experienced by a user u in a cellular system can always be split up into three parts: useful signal ($S_{b,u}$), interference and noise (N_{th}). It is common to split the system power into two terms: $I_u = I_{int,u} + I_{ext,u}$, where $I_{int,u}$ is the *internal* (or own-cell) received power and $I_{ext,u}$ is the *external* (or other-cell) interference. We consider that useful signal $S_{b,u}$ is included in the $I_{int,u}$. It should be noted that this useful signal power has to be distinguished from the commonly considered own-cell interference. In a CDMA network, the lack of orthogonality induces own-cell interference. In a OFDMA network, there is a perfect orthogonality between users and thus $I_{int,u} = S_{b,u}$.

With the above notations, the signal to interference plus noise ratio (SINR) is given by:

$$\gamma_u = \frac{P_{Tx} g_{b,u}}{\sum_{j \neq b} P_{Tx} g_{j,u} + N_{th}}, \tag{1}$$

where $g_{j,u}$ is the path-gain between BS j and user u.

Reference [4] has defined the interference factor in u, as the ratio of total power received from other BS to the total power received from the serving BS $\psi(u)$: $f_u = I_{ext,u}/I_{int,u}$. The quantities f_u, $I_{ext,u}$, and $I_{int,u}$ are location dependent and can thus be defined at any location x as long as the serving BS is known. In an OFDMA network, $I_{ext,u}$ is the total interference, and thus f_u is the inverse of the signal to interference ratio (SIR) per subcarrier. Throughout this paper, we shall neglect noise in our analytical calculations. This is a common assumption for macro-cells in dense urban areas. In this case, the SINR, γ_u can be approximated by the SIR:

$$\gamma_u \approx \frac{S_{b,u}}{I_{ext,u}} = 1/f_u.$$

As a consequence, it is clear that the approach developed in [4] can be adapted to OFDMA networks, as soon as the orthogonality factor α considered in CDMA networks is zero (details on fluid model are given in appendix). In this case, SIR per subcarrier is simply the inverse of the interference factor

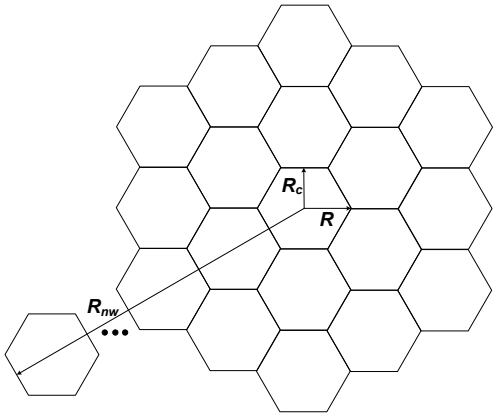

Fig. 1. Hexagonal network and main parameters of the study.

considered in [4].

$$\gamma_u = \frac{r_u^{-\eta}(\eta - 2)}{2\pi\rho_{BS}(2R_c - r_u)^{2-\eta}}. \tag{2}$$

Note that the shadowing effect is neglected in this paper. An extension of the fluid model has been proposed in [6] to take into account shadowing. The results presented in this paper can thus be extended accordingly.

We now compare the results obtained with Eq. 2 with those obtained numerically by Monte Carlo simulations. The simulator assumes an homogeneous hexagonal network made of several rings around a central cell. Fig. 1 shows an example of such a network with the main parameters involved in the study.

Fig. 2 shows the simulated SINR (using Monte Carlo simulations) as a function of the distance from the base station. Following are the simulation parameters: $R = 1$ Km, η between 2.7 and 4, $\rho_{BS} = (3\sqrt{3}R^2/2)^{-1}$, the number of rings is 15, and the number of snapshots is 3000. To include the effect of pathloss, Erceg model [14] is used: $g_{b,u} = Ar_{b,u}^{-\eta}$, such that $A = \left(\frac{4\pi d_0 f}{c d_0^{\eta/2}}\right)^2$, $d_0 = 100$ m, $f = 2.5$ GHz and c is the speed of light. Thermal noise density has been taken as -174 dBm/Hz and a subcarrier spacing of 11 KHz is considered [12]. Eq. 2 is also plotted for comparison.

In all cases, the fluid model matches very well the simulations in an hexagonal network for various values of path-loss exponent. Only in a short area around the BS, the fluid model is a little bit pessimistic, but this is not a region of primary interest for operators. It is to be noted that thermal noise was not considered in the fluid model while simulator does include its effect. However, the results of the two (fluid model and simulator) still match. It indicates that value of interference is much more pronounced as compared to that of thermal noise. Hence, neglecting thermal noise in the fluid model is a reasonable

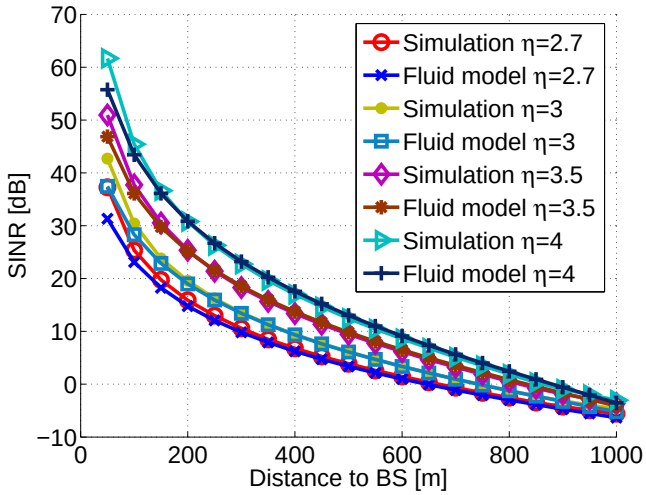

Fig. 2. SINR versus distance to the BS; comparison of the fluid model with simulations on an hexagonal network with $\eta = 2.7$, 3, 3.5, and 4 (reuse 1).

assumption.

For the rest of the paper, all above parameters are used for simulations. However, instead of different values of η, a fixed value of three is used in rest of the simulations except mentioned otherwise. The closed-form formula 2 will allow us to quickly compute performance parameters of an OFDMA network and in particular compare different reuse pattern schemes with different scheduling algorithms.

3 Integer Frequency Reuse (IFR)

In this section, we consider the application of the fluid model to IFR environments. In integer frequency reuse, all subcarriers allocated to a cell can be used anywhere in the cell without any specification of user's location. However, reutilization of subcarriers in network cells may be one or greater. An example of IFR with frequency reuse 1 is shown in Fig. 3, where W represents the available network bandwidth. For frequency reuse 1, cell bandwidth equals network bandwidth.

Two cases, frequency reuse 1 and K, have been considered. We first derive SINR and spectral efficiency expressions as functions of the distance from the BS using the fluid model. We then take into account three scheduling schemes (equal data rate, equal bandwidth and opportunist) and derive the total cell data rate for each of them. Results of analytical expressions are also compared with results of Monte Carlo simulations.

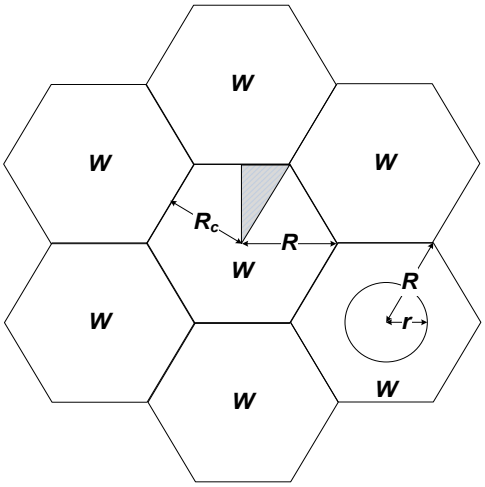

Fig. 3. Integer Frequency Reuse (IFR) case (reuse 1). Shaded triangular region shows the basic integration area.

3.1 IFR with Reuse 1

Consider Eq. 2 that gives expression for SINR of a subcarrier for a user at distance r_u. A user at distance r from BS has a specific value of SINR and spectral efficiency. Hence, in rest of the paper, subscript u is omitted for r, SINR and spectral efficiency. With $\rho_{BS} = 1/(2\sqrt{3}R_c^2)$ and introducing the normalized distance x such that $x = r/R_c$, the expression for SINR can be rewritten as:

$$\gamma_{IFR1}(x) = \frac{\sqrt{3}}{\pi}(\eta - 2)(2 - x)^{-2}(2/x - 1)^{\eta}. \tag{3}$$

For comparison between simulation and fluid model, Fig. 2 can be consulted in which all curves for fluid model have been drawn using Eq. 3.

By using Shannon's formula, spectral efficiency (in bps/Hz) as a function of variable x is given as:

$$C_{IFR1}(x) = \log_2[1 + \gamma_{IFR1}(x)], \tag{4}$$

where $\gamma_{IFR1}(x)$ is furnished by Eq. 3.

In following sections, we use this expression of spectral efficiency to calculate total cell data rate for three scheduling schemes.

3.1.1 Equal data rate

While considering equal data rate, users are assigned the bandwidth in a way that resultant data rate for every user, D_u, is the same. Higher is the distance of a user from the BS, lower is the available spectral efficiency and thus, higher is the bandwidth (or number of subcarriers) allocated to it. As SINR and spectral efficiency depend on r, let $W_u(r)$ be the bandwidth allocated by the scheduler to a user at distance r from the BS.

User data rate, D_u, can now be written for any r:

$$D_u = W_u(r)C(r), \tag{5}$$

under the constraint that total cell bandwidth W cannot be exceeded. Total bandwidth used in a cell is thus given as:

$$W = 12 \int_0^{\pi/6} \int_0^{R_c/\cos\theta} W_u(r)\rho_u \, r \, dr \, d\theta. \tag{6}$$

Integration is done over the shaded triangular region in Fig. 3 and multiplied by twelve to obtain the result over the entire hexagon cell.

If N_u is the number of users in a cell, user density is $\rho_u = N_u/(2\sqrt{3}R_c^2)$. Using Eq. 6 and 5, value of ρ_u and variable transformation r to x, user data rate is given as:

$$D_u = \frac{\sqrt{3}W/6}{N_u \int_0^{\pi/6} \int_0^{1/\cos\theta} \frac{x}{C_{IFR1}(x)} \, dx \, d\theta},$$

where $C_{IFR1}(x)$ is given by Eq. 4.

Since all users receive same data rate and there are N_u users in the cell, total cell data rate is $D_{T,IFR1} = N_u D_u$ and can be written using previous result as:

$$D_{T,IFR1} = \frac{\sqrt{3}W/6}{\int_0^{\pi/6} \int_0^{1/\cos\theta} \frac{x}{C_{IFR1}(x)} \, dx \, d\theta}. \tag{7}$$

A worth noting observation regarding Eq. 7 is that the total cell data rate neither depends upon the number of users in the cell nor upon the value of R_c.

The change of variables $\theta = z$ and $x = \frac{y}{\cos z}$, whose Jacobian is $\left|\frac{\partial(\theta,x)}{\partial(z,y)}\right| = \left|\frac{1}{\cos z}\right|$,

Table 1
Total cell data rate ($D_{T,IFR1}$) versus η (IFR reuse 1, bandwidth=10 MHz, Equal data rate).

η	$D_{T,IFR1}$ **[Mbps]**		**Difference**
	Fluid model	Simulation	
2.5	6.62	7.43	10.9%
2.6	7.83	8.26	5.21%
2.7	9.01	9.08	0.77%
2.8	10.16	9.89	2.73%
3	12.4	11.6	6.9%
3.2	14.5	13.2	9.85%
3.3	15.5	13.9	11.51%

provides the equivalent equation:

$$D_{T,IFR1} = \frac{\sqrt{3}W/6}{\int_0^{\pi/6} \int_0^1 \frac{y/\cos z}{\cos z C_{IFR1}(y/\cos z)}\, dy\, dz}.$$

To compare the above results with those of simulations, parameters of section 2 are used. We set the available network bandwidth to $W = 10$ MHz and the number of users per cell to $N_u = 30$ in simulations. In Tab. 1, total cell data rate $D_{T,IFR1}$ with both the fluid model (Eq. 7) and simulations, for various values of η, are given. The best agreement is for $\eta = 2.7$, while the difference remains below 10% for η between 2.6 and 3.2. The user data rate (D_u) can be easily obtained by dividing the total cell data rate (i.e., $D_{T,IFR1}$ in this case) by number of users (N_u) in the cell. To avoid the complexity of calculating double integral, it is also possible to integrate $W_u(r)$ over a disk, whose area equals the hexagon area. Such a disk has a radius $R_e = aR_c$, where $a = \frac{\sqrt{2\sqrt{3}}}{\pi}$. Using this approach, total cell data rate can be approximated as:

$$D_{T,IFR1} \approx \frac{\sqrt{3}W/\pi}{\int_0^a \frac{x}{C(x)}\, dx}. \tag{8}$$

For value of $\eta = 3$ and $W = 10$ MHz, data rates obtained with Eq. 7 and 8 are found to be 12.4 Mbps and 12.6 Mbps respectively with a difference of 1.6%.

3.1.2 Equal bandwidth

Equal bandwidth means that all users are assigned equal bandwidth whatever the spectral efficiency is available to them. Since users close to BS benefit from

Table 2
Total cell data rate ($D_{T,IFR1}$) versus η (IFR reuse 1, bandwidth=10 MHz, equal bandwidth).

η	$D_{T,IFR1}$ **[Mbps]**		**Difference**
	Fluid model	Simulation	
2.5	12.2	13	5.92%
2.6	14.2	14.3	0.76%
2.7	16.1	15.8	1.86%
2.8	18	17.3	4.28%
3	21.6	20.1	7.3 %
3.2	25.1	22.7	10.33%
3.3	26.8	24.5	9.43%

higher spectral efficiency, they will attain a higher data rate as compared to users at cell edge. Let W_u denote the bandwidth allocated to each user such that $W = N_u W_u$. Data rate of a user at a distance r is then given as:

$$D_u(r) = W_u C(r), \tag{9}$$

total data rate then can be obtained by integrating the user data rates over cell surface:

$$D_{T,IFR1} = 12 \int_0^{\pi/6} \int_0^{R_c/\cos\theta} D_u(r)\rho_u \, r \, dr \, d\theta, \tag{10}$$

using Eq. 9, user density $\rho_u = N_u/(2\sqrt{3}R_c^2)$, user bandwidth $W_u = N_u/W$ and transformation of variable r to x, we get:

$$D_{T,IFR1} = \frac{6W}{\sqrt{3}} \int_0^{\pi/6} \int_0^{1/\cos\theta} x C_{IFR1}(x) \, dx \, d\theta. \tag{11}$$

The simulation and fluid model results are compared in Tab. 2.

3.1.3 Opportunist

In opportunist scheduling, user experiencing the greatest SINR is assigned all the resources and rest of the users receive no resources at all. In light of assumptions considered in this paper, user closest to the BS will have the

maximum SINR value. To calculate the total cell data rate for opportunist scheduling, we require PDF (probability density function) of the distance, X, of the user nearest to the BS. For N_u users in the cell, the CDF of X is given by:

$$F_X(r) = p[X \leq r] = 1 - p[X > r] = 1 - (1 - \pi r^2 / 2\sqrt{3} R_c^2)^{N_u},$$

and its PDF can be obtained by differentiating the CDF:

$$p_{X,IFR}(r) = \frac{\pi N_u r}{\sqrt{3} R_c^2} \left(1 - \frac{\pi r^2}{2\sqrt{3} R_c^2}\right)^{N_u - 1},$$

with change of variable from r to x, the PDF for IFR over small distance dx can be rewritten as:

$$p_{X,IFR}(x)dx = \frac{\pi N_u x}{\sqrt{3}} \left(1 - \frac{\pi x^2}{2\sqrt{3}}\right)^{N_u - 1} dx, \tag{12}$$

taking into account the circular disc of radius $R_e = aR_c$ with $a = \frac{\sqrt{2\sqrt{3}}}{\pi}$ (refer section 2) the average cellular spectral efficiency for opportunist scheduling can be calculated using following equation:

$$\bar{C}_{IFR1} = \int_0^a C_{IFR1}(x) p_{X,IFR}(x)\, dx.$$

Finally total cell data rate is written as:

$$D_{T,IFR1} = W \bar{C}_{IFR1}.$$

To verify this approach, simulations are carried out with $N_u = 30$. The results of simulation and model are given in Tab. 3.

3.2 IFR with Reuse K

For IFR with reuse higher than one, analytical study is very similar to the previous one. The difference lies in the fact that only co-channel BS are considered in interference calculation and thus the half-distance between base stations and BS density have to be modified. As a consequence, previous analysis results are still valid provided that R_c is replaced by $\sqrt{K} R_c$ and BS density is divided by K, i.e., ρ_{BS} is replaced by ρ_{BS}/K. Hence using Eq.2 and this new half distance between BS, SINR is given as:

$$\gamma(r) = \frac{r^{-\eta}(\eta - 2)}{2\pi \cdot \frac{\rho_{BS}}{K} (2\sqrt{K} R_c - r)^{2-\eta}}. \tag{13}$$

Table 3
Total cell data rate ($D_{T,IFR1}$) versus η (IFR reuse 1, bandwidth=10 MHz, opportunist).

η	$D_{T,IFR1}$ **[Mbps]**		**Difference**
	Fluid model	Simulation	
2.5	56.6	56.9	0.48%
2.6	62.8	61.6	1.95 %
2.7	68.5	66.5	3%
2.8	74	71.5	3.6%
3	84.5	80.3	5.2%
3.2	94.4	89.2	5.9%
3.3	99.3	93.8	5.8%

Using the same distance normalization as before (leading to the transformation of variable r to x) and after few manipulations, SINR can be written as:

$$\gamma_{IFRK}(x) = \frac{K\sqrt{3}}{\pi}(\eta - 2)(2\sqrt{K} - x)^{-2}(2\sqrt{K}/x - 1)^{\eta}. \tag{14}$$

Hence spectral efficiency (in bps/Hz) for IFR reuse K can be given as:

$$C_{IFRK}(x) = \log_2[1 + \gamma_{IFRK}(x)]. \tag{15}$$

To validate above approach, reuse 3 is considered as an example. Plot of SINR versus distance to BS for reuse 3 case, for both fluid model and simulation, is shown in Fig. 4. As expected SINR is higher than for reuse 1. However, bandwidth per cell equals one third the network bandwidth. Again, both analysis and simulation provide similar results. The fluid model is thus accurate not only for reuse 1 networks but also for higher reuse factors provided the parameters are adjusted.

As far as total cell data rate for three scheduling schemes is concerned, method used for IFR reuse 1 is still valid provided that $C_{IFR1}(x)$ is replaced by C_{IFR3} (Eq. 15) and cell bandwidth is divided by 3, in all calculations. Values of total cell data rate for fluid model and simulations are shown in Tab. 4, 5 and 6. In all cases, the difference between simulation and fluid model remains below 10% for η between 2.6 and 3.5.

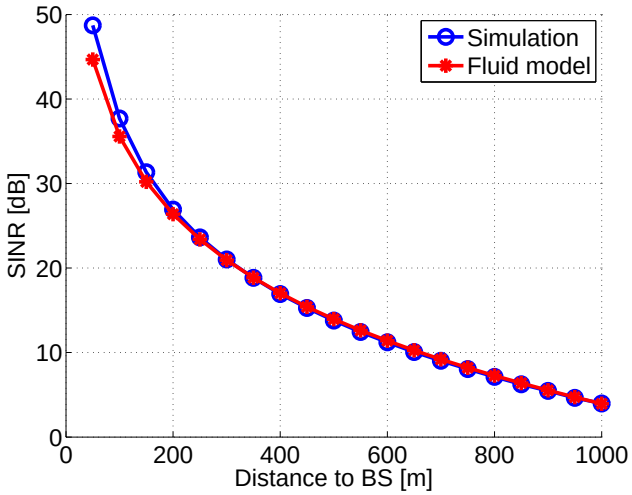

Fig. 4. SINR versus distance to BS for IFR with reuse 3.

Table 4
Total cell data rate ($D_{T,IFR3}$) versus η (IFR reuse 3, BW=10/3 MHz, equal data rate).

η	$D_{T,IFR3}$ [Mbps]		**Difference**
	Fluid model	Simulation	
2.5	6.4	7.2	11.11%
2.6	7.55	7.95	5.03%
2.7	8.66	8.73	0.8%
2.8	9.74	9.55	1.99%
3	11.8	11.2	5.36%
3.1	12.8	12.0	6.67%
3.2	13.8	12.8	7.81%
3.5	16.7	15.2	9.87%

4 Fractional Frequency Reuse (FFR)

An example of FFR scenario is depicted in Fig. 5. As can be seen in the figure, cell space is divided into two regions, inner and outer. Inner region is a circular disc with radius $R_0 \leq R_c$ and rest of the hexagon space forms the outer region. Bandwidth is allocated to inner and outer in a way that former incorporates frequency reuse 1 while the latter applies frequency reuse 3. As can be seen in Fig. 5, the network bandwidth W is equal to $W_0 + W_1 + W_2 + W_3$. It is also considered that $W_1 = W_2 = W_3$.

SINR versus distance with $R_0 = 0.7R_c$ for fluid model and simulation is given

Table 5
Total cell data rate ($D_{T,IFR3}$) versus η (IFR reuse 3, bandwidth=10/3 MHz, equal bandwidth).

η	$D_{T,IFR3}$ **[Mbps]**		**Difference**
	Fluid model	Simulation	
2.5	8.38	9.04	7.38%
2.6	9.63	9.91	2.81%
2.7	10.8	10.76	0.71%
2.8	12	11.7	3.04%
3	14.2	13.4	5.9%
3.1	15.3	14.4	6.55%
3.2	16.4	15.2	7.46%
3.5	19.4	17.8	8.8%

Table 6
Total cell data rate ($D_{T,IFR3}$) versus η (IFR reuse 3, bandwidth=10/3 MHz, opportunist).

η	$D_{T,IFR3}$ **[Mbps]**		**Difference**
	Fluid model	Simulation	
2.5	25.4	26	2.2%
2.6	27.8	28.0	0.7%
2.7	30	29.6	1.3%
2.8	32.2	31.5	2%
3	36.2	34.7	4.3%
3.1	38.2	36.6	4.4%
3.2	40.1	38.2	5.1%
3.5	45.7	43.4	5.4%

in Fig.6. As expected FFR scheme improves radio quality at cell edge. Moreover, the results follow the previous positive trend, i.e., fluid model and simulations are in conformity.

Now we derive the expressions for total cell data rate assuming schedulers fair in throughput, fair in resource allocation and opportunist. We also estimate the optimized inner region radius.

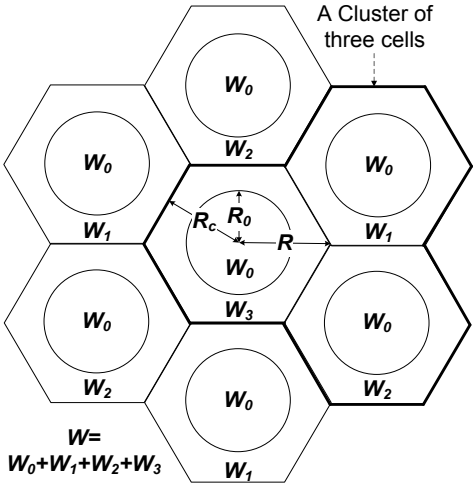

Fig. 5. Fractional Frequency Reuse (FFR) case. Bandwidth W_0 is used to deploy reuse 1 between inner regions, while W_1, W_2 and W_3 are used to deploy reuse 3 between outer regions.

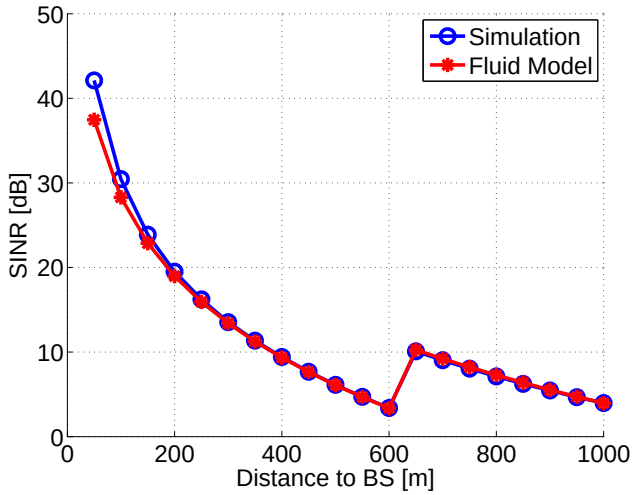

Fig. 6. SINR versus distance to BS for FFR with $R_0 = 0.7R_c$.

4.1 Equal data rate

To carry out total cell data rate, we first consider the inner circular region. Since for this region, frequency reuse is 1, the expression of SINR is given by Eq. 2 or equivalently by Eq. 3. Once again, it is considered that users are uniformly distributed in the cell space with $\rho_u = N_u/2\sqrt{3}R_c^2$. Since it is a circular region, the elementary area ds of Eq. **??** can be simply taken as $2\pi r dr$ and the bandwidth of inner region is given as:

$$W_0 = \int_0^{R_0} W_u(r)\rho_u \, 2\pi r \, dr. \tag{16}$$

After replacing ρ_u by its value, transformation of variable r to x and using Eq. 5, we get

$$W_0 = \frac{\pi}{\sqrt{3}} D_u N_u \int_0^{R_0/R_c} \frac{x}{C_{IFR1}(x)}\, dx,$$

where $C_{IFR1}(x)$ is given by Eq.4. Let I_0 be the integral in the previous expression, so that $W_0 = \pi/\sqrt{3} I_0 D_u N_u$.

Let us now consider the outer area, which applies reuse 3. SINR for reuse 3 is given by Eq. 13 or equivalently by Eq. 14. In order to calculate the total bandwidth used in the outer region, double integral used in Eq. 6 is applied with change of limits and replacing $W_u(r)$ by $W_{1,u}(r)$ we get:

$$W_1 = 12 \int_0^{\pi/6} \int_{R_0}^{R_c/\cos\theta} W_{1,u}(r) \rho_u\, r\, dr\, d\theta,$$

where $W_{1,u}(r)$, assuming equal data rate, is given as: $W_{1,u}(r) = D_u C_{IFR3}(r)$. After replacing ρ_u by its value and transformation of variable r to x, we get

$$W_1 = \frac{6}{\sqrt{3}} D_u N_u \int_0^{\pi/6} \int_{R_0/R_c}^{1/\cos\theta} \frac{x}{C_{IFR3}(x)}\, dx\, d\theta. \tag{17}$$

Let I_1 be the double integral in the previous expression, so that $W_1 = \frac{6}{\sqrt{3}} I_1 D_u N_u$.

Considering the fact that total network bandwidth is W with $W = W_0 + W_1 + W_2 + W_3$ and $W_1 = W_2 = W_3$ we can write: $W = W_0 + 3 \times W_1$. Finally using Eq. 16 and 17 and keeping in view that $D_T = D_u N_u$ we get expression of the total cell data rate $D_{T,FFR}$ for FFR case:

$$D_{T,FFR} = \frac{\sqrt{3} W}{\pi I_0 + 18 I_1}. \tag{18}$$

Total cell data rate calculation also shows that fluid model and simulation differ by 5.6% with values of 13.2 Mbps and 12.5 Mbps respectively for 10 MHz of network bandwidth. Fig.7 shows the total cell data rate as a function of the inner cell radius R_0. Both fluid model and simulations provide an optimum value of approximately 757 m.

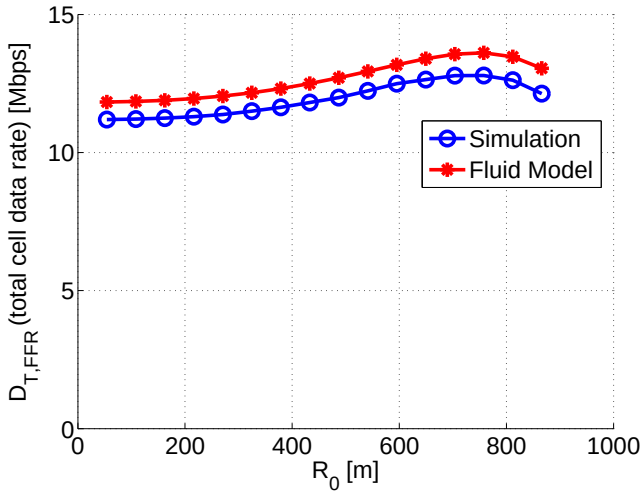

Fig. 7. $D_{T,FFR}$ (total cell data rate) versus radius of inner region with equal data rate for FFR scheme. Maximum value occurs at $R_0 = 757\ m$ approx.

4.2 Equal Bandwidth

To calculate cell data rate in this case, we adopt the same approach as was used in section 3.1.2 while considering $N_u W_u = W_0 + W_1$. By integrating the user data rate over inner circular region (using frequency reuse 1), total data rate of inner region is given by Eq. 19.

$$D_{T,Inner} = \frac{\pi(W_0 + W_1)}{\sqrt{3}} \int_0^{R_0/R_c} x C_{IFR1}(x)\, dx. \tag{19}$$

Similarly, assuming frequency reuse 3 for the outer region, total data rate of outer region is:

$$D_{T,Outer} = \frac{6(W_0 + W_1)}{\sqrt{3}} \int_0^{\pi/6} \int_{R_0/R_c}^{1/\cos\theta} x C_{IFR3}(x)\, dx\, d\theta, \tag{20}$$

and total cell data rate is the sum of inner and outer region data rates:

$$D_{T,FFR} = D_{T,Inner} + D_{T,Outer}. \tag{21}$$

Since this scheduling scheme assigns equal resources to all users (whether located in inner or outer region), the ratio of W_0 to W_1 should be proportional to number of users in two regions. But as we have assumed that users are uniformly distributed in cell space, this ratio should be equal to ratio of inner

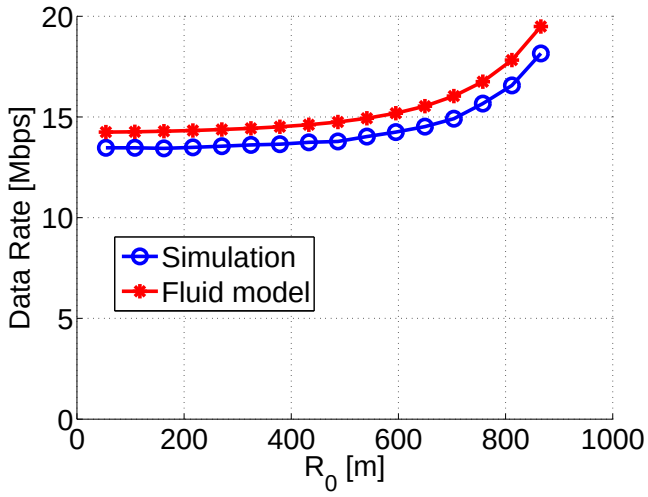

Fig. 8. $D_{T,FFR}$ (total cell data rate) versus radius of inner region with equal bandwidth for FFR scheme. Maximum value occurs at $R_0 = R_c$.

region area to outer region area:

$$\frac{W_1}{W_0} = \frac{2\sqrt{3}R_c^2}{\pi R_0} - 1, \tag{22}$$

and since $W_0 + 3W_1 = W$, it can be shown that:

$$W_1 = \frac{2\sqrt{3}R_c^2 - \pi R_0^2}{6\sqrt{3}R_c^2 - 2\pi R_0^2} W. \tag{23}$$

It can be made out from Eq. 23 that for every value of R_0, there is a specific value of W_1 and hence W_0. For different values of R_0, total cell data rate has been plotted in Fig. 8. It can be seen that maximum value of total cell data rate is for $R_0 = R_c$.

Tab. 2 and 5 have shown that IFR1 provides higher data rates than IFR3. In FFR, increasing R_0 and thus the bandwidth W_0 used with reuse 1, makes FFR closer to IFR1. On the contrary, decreasing R_0 makes FFR closer to IFR3. As a consequence, total cell data rate is maximized for the highest value of R_0.

4.3 Opportunist

For opportunist scheduling in FFR case, we assume that two users are simultaneously scheduled in a cell such that one user having the greatest SINR among inner region users and other one having the highest SINR among outer region users. If there is no user in any of the regions, bandwidth of that region

goes unallocated. Following the methodology of section 3.1.3, for the inner region, PDF of the user's (nearest to the BS) distance, knowing there are $N_{u,i}$ users located in the inner region is given as:

$$p_{X,inner|N_{u,i}}(r) = \frac{2rN_{u,i}}{R_0^2}\left(1-\frac{r^2}{R_0^2}\right)^{N_{u,i}-1},$$

or with substitution of r by x, the same PDF over small distance dx can be written as:

$$p_{X,inner|N_{u,i}}(x)\,dx = \frac{2xN_{u,i}}{(R_0/R_c)^2}\left(1-\frac{x^2}{(R_0/R_c)^2}\right)^{N_{u,i}-1}dx.$$

Hence, the average spectral efficiency of inner region, given that there are $N_{u,i}$ located inside it, can be expressed by the following integral:

$$\bar{C}_{FFR,inner|N_{u,i}} = \int_0^{R_0/R_c} C_{IFR1}(x)p_{X,inner|N_{u,i}}(x)\,dx.$$

Similarly for the outer region, PDF of the user's (nearest to the BS) distance, knowing there are $N_{u,i}$ users located in the inner region is given as:

$$p_{X,outer|N_{u,i}}(r) = \frac{2\pi(N_u-N_{u,i})r}{2\sqrt{3}R_c^2-\pi R_0^2}\left(1-\frac{\pi r^2-\pi R_0^2}{2\sqrt{3}R_c^2-\pi R_0^2}\right)^{N_u-N_{u,i}-1},$$

where $(N_u - N_{u,i})$ is the number of users in the outer region.

Once again with change of variable r to x, the PDF over small distance dx for outer region can be expressed as:

$$p_{X,outer|N_{u,i}}(x)\,dx = \frac{2\pi(N_u-N_{u,i})x}{2\sqrt{3}-\pi(R_0/R_c)^2}\left(1-\frac{\pi x^2-\pi(R_0/R_c)^2}{2\sqrt{3}-\pi(R_0/R_c)^2}\right)^{N_u-N_{u,i}-1}dx,$$

and the average spectral efficiency for the outer region such that there are $N_{u,i}$ users in the inner region is given by following equation:

$$\bar{C}_{FFR,outer|N_{u,i}} = \int_{R_0/R_c}^{a} C_{IFR3}(x)p_{X,outer|N_{u,i}}(x)\,dx.$$

Note that in this latter equation, we approximate the hexagon by a disk of radius R_e. Finally, averaging the sum of data rates (of inner and outer regions)

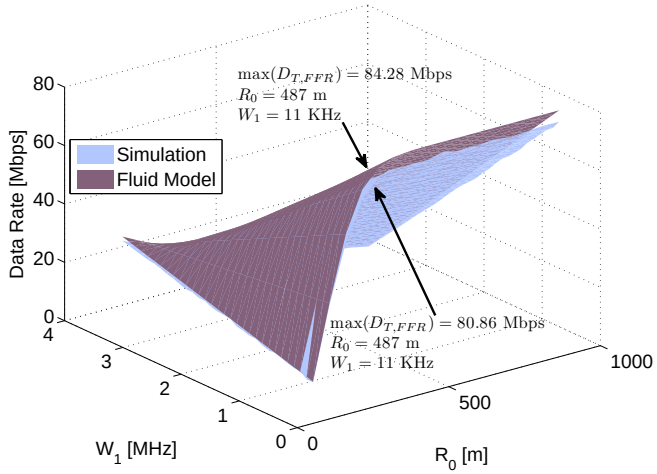

Fig. 9. $D_{T,FFR}$ (total cell data rate) versus radius of inner region and versus versus bandwidth allocated in the outer region with opportunist scheduling for FFR scheme. Maximum value occurs at $R_0 = 487$ m and $W_1 = 11$ KHz.

for all possible values of $N_{u,i}$ results in total cell data rate for FFR case:

$$D_{T,FFR} = \sum_{N_{u,i}=0}^{N_u} (W_0 \bar{C}_{FFR,inner|N_{u,i}} + W_1 \bar{C}_{FFR,outer|N_{u,i}}) P[N_{u,i}],$$

where $P[N_{u,i}]$ is the probability that there are $N_{u,i}$ out of N_u users in the inner region:

$$P[N_{u,i}] = \left(\frac{\pi R_0^2}{2\sqrt{3}R_c^2}\right)^{N_{u,i}} \left(1 - \frac{\pi R_0^2}{2\sqrt{3}R_c^2}\right)^{N_u - N_{u,i}} \binom{N_u}{N_{u,i}}.$$

The total cell data rate (for FFR scheme) as a function of different values of W_1 and R_0 is shown in Fig. 9. Maximum value of total cell data rate can be observed for a value of $W_1 = 11$ KHz (i.e., one subcarrier) and $R_0 = 487$ m for both the simulation and fluid model. The maximum difference between simulation and analytical model results for all values of W_1 and R_0 is found to be 6.7%.

5 Two Level Power Control (TLPC)

In previous section, we discussed the concept of FFR in OFDMA and we have shown that SINR could be improved by using a reuse 3 pattern in cell outer regions. With FFR, it is however not possible to use full network bandwidth in a cell, which reduces the overall cell bandwidth.

To overcome this drawback, it is possible to adopt a reuse 1 pattern while using a two level power control (TLCP) mechanism to improve the radio quality in

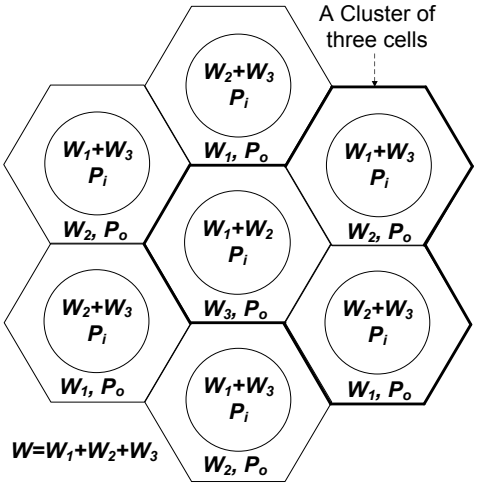

Fig. 10. Two level power control case. Bandwidth W is partitioned into three equal parts, i.e., $W_1 = W_2 = W_3$

the outer region. The TLPC scheme is shown in Fig.10. Total bandwidth in a cell (equal to network bandwidth) is divided into three equal parts: two parts allocated to inner region and one to the outer region. The output power per subcarrier in the inner region is P_i and that in the outer region is P_o. These two values of power are related as: $P_o = \delta P_i$, such that $\delta \geq 1$. The three spectrum parts W_1, W_2 and W_3 alternate from cell to cell in such a way that there is a pseudo-reuse 3 scheme between outer regions. Neighboring cells contribute in fact to interference in the outer region but with a reduced power P_i. The consequence is that the total network bandwidth is used in every cell but interference is expected to be reduced in outer regions.

Let us calculate SINR for inner and outer region of this two level power control network. For a user in the outer region (using e.g. W_3 in the center cell in Fig.10), we divide the interference into two categories. One is from the cells using same subcarriers in the outer region and we represent it by I_{outer}. Other is from cells using same subcarriers in the inner region (neighboring cells) and is represented by I_{inner}. Then, SINR for a subcarrier in the outer region can be written as:

$$\gamma_{TLPC,outer}(r) = \frac{P_o A r^{-\eta}}{I_{inner} + I_{outer}}.$$

With slight change of form, the above expression can be rewritten as:

$$\frac{1}{\gamma_{TLPC,outer}} = \frac{I_{inner}}{P_o A r^{-\eta}} + \frac{I_{outer}}{P_o A r^{-\eta}}. \tag{24}$$

In order to find the values of I_{inner} and I_{outer}, consider that $\mathcal{B}_{outer}$ represents the set of BS causing I_{outer}. For a user u in outer region of a cell b, I_{outer} is

given as:

$$I_{outer} = P_o A \sum_{j=1, j\in\mathcal{B}_{outer}}^{N_{BS}} r_{j,u}^{-\eta}. \tag{25}$$

As outer regions of BS in $\mathcal{B}_{outer}$ form together a reuse 3 scheme, the second term of right hand side of Eq. 24 is simply $1/\gamma_{IFR3}$.

Adding up the interference from all network cells, I_{inner} can be written as:

$$I_{inner} = P_i A \sum_{j=1, j\neq b}^{N_{BS}} r_{j,u}^{-\eta} - P_i A \sum_{j=1, j\in\mathcal{B}_{outer}}^{N_{BS}} r_{j,u}^{-\eta}. \tag{26}$$

Thus, considering $\delta = P_o/P_i$:

$$\frac{I_{inner}}{P_o A r^{-\eta}} = \frac{1}{\delta}\frac{1}{\gamma_{IFR1}} - \frac{1}{\delta}\frac{1}{\gamma_{IFR3}}. \tag{27}$$

Combining previous results, we can rewrite Eq. 24 as:

$$\frac{1}{\gamma_{TLPC,outer}} = \frac{1}{\delta}\frac{1}{\gamma_{IFR1}} + (1 - \frac{1}{\delta})\frac{1}{\gamma_{IFR3}}. \tag{28}$$

Now we find out SINR expression for inner region. Consider the central cell of Fig. 10, in which W_1 and W_2 are allocated to inner region and W_3 is used in the outer region. A user in inner region will be allocated a subcarrier that will either belong to W_1 or W_2. If we look at the bandwidth utilized in the six neighboring cells of center cell, we notice that out of six, three are transmitting on the same subcarrier with power P_o, while other three with P_i. Hence, SINR for this inner region subcarrier can be approximated while considering that neighboring cells transmit with average power $(P_i + P_o)/2$ and

$$\gamma_{TLPC,inner}(r) \approx \frac{P_i A r_{b,u}^{-\eta}}{\frac{P_o+P_i}{2} A \sum_{j=1, j\neq b}^{N_{BS}} r_{j,u}^{-\eta}} = \frac{2}{1+\delta}\gamma_{IFR1}. \tag{29}$$

Using the values of SINR for outer and inner region, spectral efficiencies for two regions are given in Eq. 30 and 31.

$$C_{TLPC,inner} = \log_2(1 + \gamma_{TLPC,inner}), \tag{30}$$

$$C_{TLPC,outer} = \log_2(1 + \gamma_{TLPC,outer}). \tag{31}$$

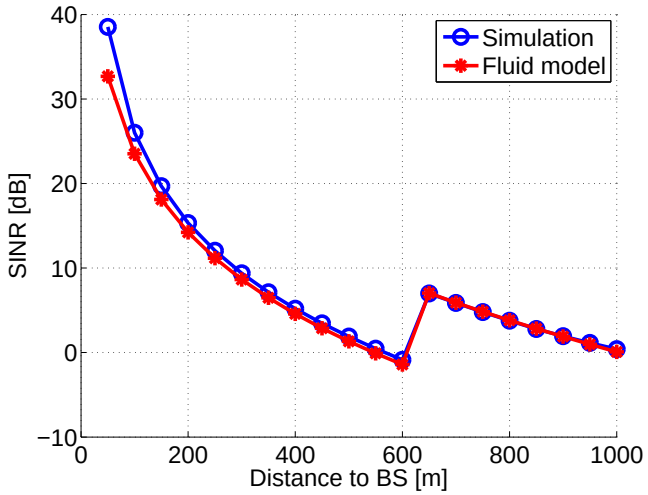

Fig. 11. SINR versus distance to BS for TLPC scheme with $R_0 = 0.7R_c$ and $\delta = 5$.

To verify the above results, SINR versus distance (with $R_0 = 0.7R_c$ and $\delta = 5$) is given in Fig. 11. As expected, radio quality is improved in outer region with TLPC compared to the IFR1 case in a similar way FFR does. Let us now compare total cell data rates.

In order to calculate data rate for inner and outer region for three scheduling schemes, we assume that in Fig. 10, $W_1 = W_2 = W_3$. We start with equal data rate scheduling scheme.

5.1 Equal Data Rate

Using the similar approach of section 4, we can write:

$$W_1 + W_2 = \frac{2W}{3} = \frac{\pi}{\sqrt{3}} D_{u,inner} N_u \int_0^{R_0/R_c} \frac{x dx}{C_{TLPC,inner}(x)},$$

and

$$W_3 = \frac{W}{3} = \frac{6}{\sqrt{3}} D_{u,outer} N_u \int_0^{\pi/6} \int_{R_0/R_c}^{1/\cos\theta} \frac{x}{C_{TLPC,outer}(x)} \, dx \, d\theta.$$

Using above two equations, we can write the ratio between data per user for inner and outer region as:

$$\frac{D_{u,inner}}{D_{u,outer}} = \frac{12}{\pi} \frac{\int_0^{\pi/6} \int_{R_0/R_c}^{1/\cos\theta} \frac{x}{C_{TLPC,outer}(x)} \, dx \, d\theta}{\int_0^{R_0/R_c} \frac{x}{C_{TLPC,inner}(x)} \, dx}.$$

Now, if we assume a scheduler fair in throughput, $\frac{D_{u,inner}}{D_{u,outer}}$ should be equal to

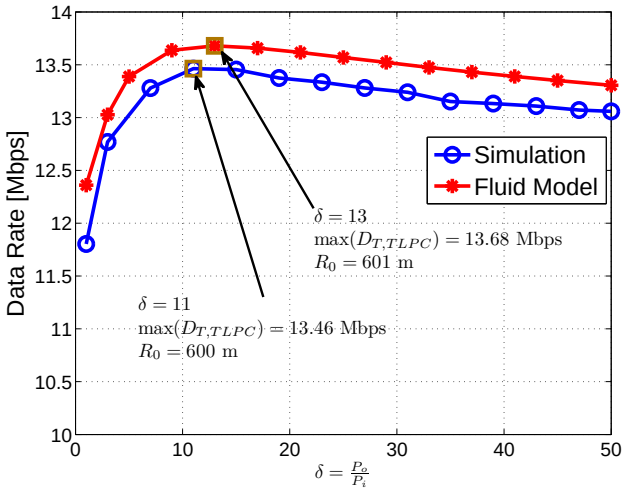

Fig. 12. Total cell data rate versus different values of δ with equal data rate for TLPC scheme.

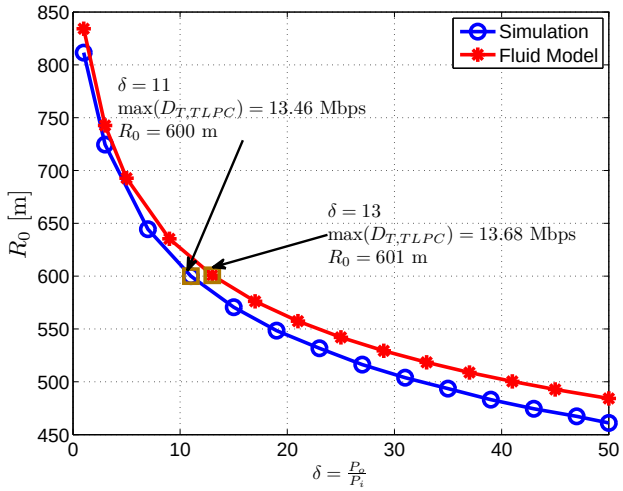

Fig. 13. R_0 (radius of inner region that guarantees equal data rate among users) versus different values of δ for TLPC scheme.

one. For a given value of δ there exists a unique value of R_0 for which above condition is satisfied. In Fig. 12, total cell data rate satisfying equal data rate has been plotted for various values of δ. It is clear that for small values of δ, total cell data rate increases with increasing values of δ. The total cell data rate attains its maximum value of 13.68 Mbps for $\delta = 13.2$. Beyond $\delta = 13.2$ (or 11.2 dB), the total cell data rate starts decreasing. The corresponding values of R_0 for these total cell data rates are given in Fig. 13. The figure shows R_0 is a decreasing function of δ. The value of R_0 corresponding to maximum value of cell data rate is approx. 600 m.

5.2 Equal bandwidth

With equal bandwidth allocation, the bandwidth of inner and outer regions should be proportional to areas of the two regions (cf. section 4.2) and since for TLPC schemes bandwidth of inner and outer region are fixed, there exists a unique value of R_0 satisfying the two conditions.

$$\frac{W_3}{W_1 + W_2} = \frac{2\sqrt{3}R_c^2}{\pi R_0^2} - 1,$$

with $W_1 = W_2 = W_3 = W/3$,

$$R_0 = \frac{2}{\sqrt{\pi\sqrt{3}}} R_c.$$

Now the total data rate of inner region is given by Eq. 32:

$$D_{T,Inner} = \frac{\pi W}{\sqrt{3}} \int_0^{R_0/R_c} x C_{TLPC,inner}(x)\, dx. \tag{32}$$

Similarly total data rate for outer region is given as:

$$D_{T,Outer} = \frac{6W}{\sqrt{3}} \int_0^{\pi/6} \int_{R_0/R_c}^{1/\cos\theta} x C_{TLPC,outer}(x)\, dx\, d\theta. \tag{33}$$

Total cell data rate is the sum of total data rates of two regions:

$$D_{T,TLPC} = D_{T,Inner} + D_{T,Outer}. \tag{34}$$

A comparison of simulation and fluid model $D_{T,TLPC}$ values, as function of δ values, is shown in Fig. 14 which shows a close proximity between the two curves.

5.3 Opportunist

The computation of cell data rate is similar to the method used in section 4.3. However, in this case, inner bandwidth is $2W/3$, outer bandwidth is $W/3$ and average spectral efficiency for TLPC is used:

$$D_{T,TLPC} = \sum_{N_{u,i}=0}^{N_u} \left(\frac{2W}{3}\bar{C}_{TLPC,inner|N_{u,i}} + \frac{W}{3}\bar{C}_{TLPC,outer|N_{u,i}}\right) P[N_{u,i}].$$

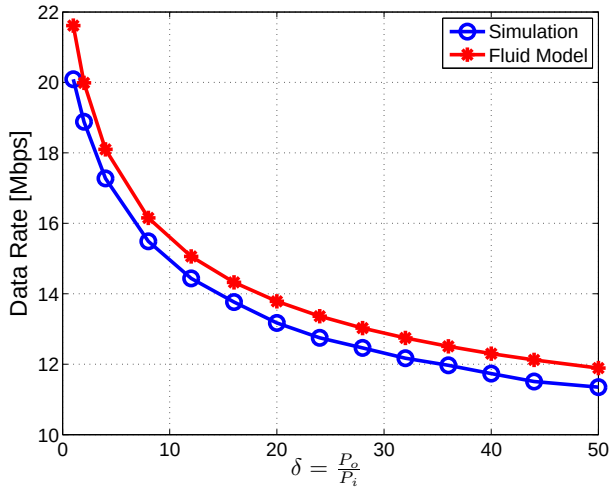

Fig. 14. Total cell data rate versus different values of δ with equal bandwidth for TLPC scheme.

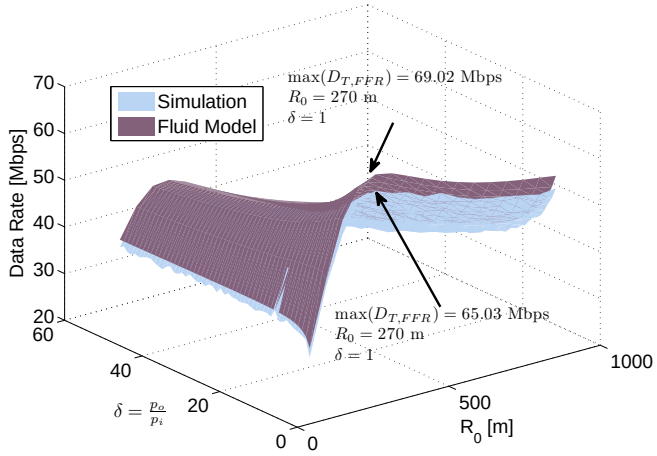

Fig. 15. $D_{T,TLPC}$ (total cell data rate) versus radius of inner region and δ with opportunist scheduling for TLPC scheme. Maximum value occurs at $R_0 = 270$ m and $\delta = 1$.

The results of simulation and fluid model are compared in Fig. 15. Total cell data rates are plotted as function of R_0 and δ. The maximum cell data rate is found to be for $R_0 = 270$ m and $\delta = 1$ for both the simulation and fluid model. The maximum difference between the values of total cell data rates with simulation and fluid model is 7.23%.

6 Comparison of reuse schemes and scheduling policies

In previous sections, we have established through validation that analytical approach based on the fluid model can be used for IFR, FFR and TLPC

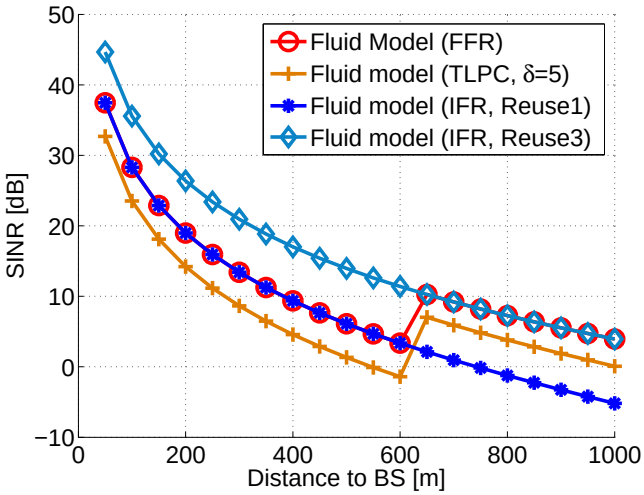

Fig. 16. SINR versus distance to BS for three reuse schemes.

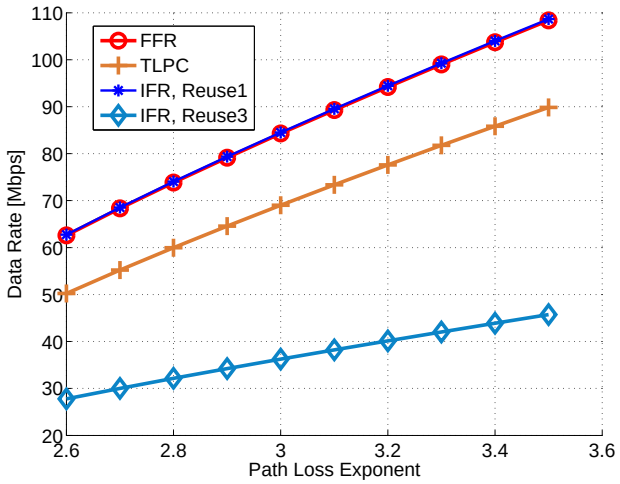

Fig. 17. Data rate versus pathloss exponent with opportunist scheduling for three reuse schemes.

schemes while considering three different scheduling types: equal data rate, equal bandwidth and opportunist. In this section, we present a comparison between these three reuse schemes and the three scheduling policies by applying fluid model.

If we look at Fig. 16, it can be deduced that IFR with reuse 3 shows the best performance in terms of SINR values. IFR reuse 1 is much lower than IFR reuse 3 in terms of radio quality. FFR exactly follows IFR reuse 1 curve until R_0 and IFR reuse 3 onwards. Compared to IFR reuse 1, TLPC improves SINR in outer region at the expense of a degraded radio quality in inner region.

We now compare total cell data rates for all frequency reuse schemes in presence of three scheduling algorithms. Total cell data rates in FFR may depend upon value of R_0 and W_1. The same applies to TLPC w.r.t. parameters R_0

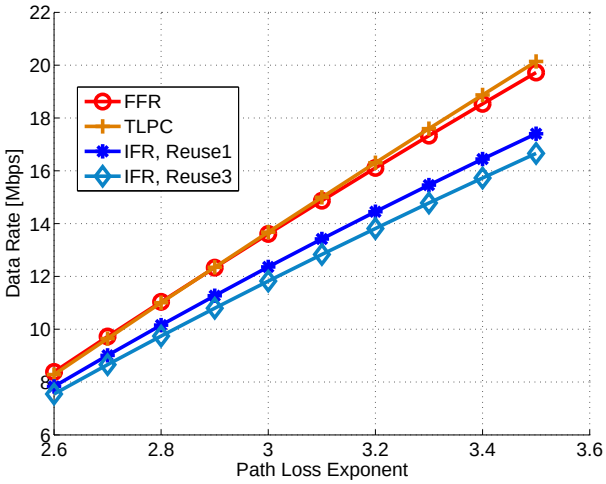

Fig. 18. Data rate versus pathloss exponent with equal data rate scheduling for three reuse schemes.

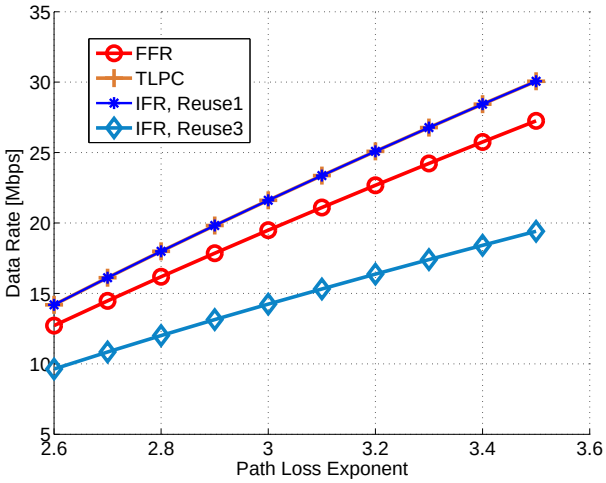

Fig. 19. Data rate versus pathloss exponent with equal bandwidth scheduling for three reuse schemes.

and δ. For these two schemes, maximum possible value of total cell data rate, based on optimal values of their parameters, has been considered in the comparison. These optimal values are presented aside with values of data rates (see Tab. 7).

The value of network bandwidth is 10 MHz. Number of users per cell N_u is considered to be thirty in all cases. Path loss constant η is taken as three. Results of cell data rate are listed in Tab. 7.

With equal data rate, IFR3 touches the lowest performance although SINR values are greater. This is due to the fact that utilization of network bandwidth per cell is lower as compared to other schemes. TLPC has the maximum value with $\delta = 13.2$ and has a comparable performance w.r.t. FFR (with $R_0 = 757$ m). Hence, by applying TLPC and FFR schemes, we can diminish

Table 7
Total cell data rate (D_T) comparison of three reuse schemes and three scheduling policies.

Frequency Reuse Scheme	**D_T [Mbps]**		
	equal data rate	equal bandwidth	opportunist ($N_u = 30$)
FFR	13.61 ($R_0 = 757\ m$)	19.5 ($R_0 = R_c$)	84.28 ($W_1 = 11$ KHz, $R_0 = 487$ m)
TLPC	13.68 ($\delta = 13.2, R_0 = 600$ m)	21.6 ($\delta = 1$, $R_0 = 742$ m)	69.02 ($\delta = 1, R_0 = 270$ m)
IFR, Reuse 1	12.4	21.6	84.5
IFR, Reuse 3	11.8	14.2	36.2

the problem of reduced radio quality (SINR) in case of IFR1. At the same time, bandwidth is more efficiently utilized than with IFR3. Due to its simplicity, FFR could be preferred to TLPC with equal data rate scheduling.

An equal bandwidth scheduling aims at improving resource utilization (compared to equal data rate scheduling) while ensuring resources to every user (on the contrary to opportunist scheduling). So, for all reuse schemes, total cell data rate is in-between two other schemes. With equal bandwidth, IFR1 achieves the highest cell capacity because it benefits from the usage of total network bandwidth in every cell. Although SINR are higher with IFR3, this scheme allocates only one third of the total network bandwidth to each cell, this explains again the lower achieved performance.

FFR and TLPC cannot do better than IFR1 and reach their maximum value for a parameter set that makes them very close to IFR1. With FFR, setting $R_0 = R_c$ makes most of the bandwidth to be used with reuse 1. A higher radio quality at cell border is obtained at the price of a small reduction of the total cell data rate compared to IFR1. With TLPC, setting $\delta = 1$ reduces almost this scheme to IFR1.

Total cell data rate obtained with opportunist scheduling provides an upper bound (for a given number of users) on the cell performance at the price of fairness. Except in TLPC, only the best user is served and gets the whole bandwidth. IFR1 achieves again the highest cell data rate. FFR tends towards IFR1 with very small bandwidth being allocated to the outer region. The choice of scheduling two users (one in the inner region, one in the outer) reduces the performance of TLPC compared to IFR1 since part of the bandwidth is allocated to a user a bit far from the BS.

7 Conclusions

In this paper, we have presented an analytical approach, based on the fluid model, for analyzing OFDMA based networks. We have shown that our proposed technique is very flexible and can be used in different frequency reuse scenarios. We have introduced expressions of SINR and cell data rate for IFR, FFR and TLPC schemes and taking into account equal data rate, equal bandwidth and opportunist scheduling types. We have also validated our technique by comparing its results with those obtained from Monte Carlo simulations. Time required to obtain results with our analytical technique is however much shorter. We have shown that our proposed technique gives a fairly good performance for η values between 2.6 and 3.5 which is a range found in most of practical scenarios. A comparison of above three schemes is also provided. For each scheduling type, we have shown which frequency reuse scheme provides the maximum cell data rate.

8 Acknowledgments

This work was prepared through collaborative participation in the URC: Urban Planning for Radio Communications project, sponsored by the System@tic Paris-Région Cluster.

Authors would also like to thank Trung Dung Nguyen, student at ENST, whose project [11] under the supervision of Philippe Godlewski formed the first step in carrying out this work.

References

[1] Mobile WiMAX-Part II: A Comparative Analysis, Tech. rep., WiMAX Forum (May 2006).

[2] C. He, F. Liu, H. Yang, C. Chen, H. Sun, W. May, J. Zhang, Co-channel Interference Mitigation in MIMO-OFDM System, in: Proc. of IEEE WiCom, 2007.

[3] H. Jia, Z. Zhang, G. Yu, P. Cheng, S. Li, On the Performance of IEEE 802.16 OFDMA System under Different Frequency Reuse and Subcarrier Permutation Patterns, in: Proc. of IEEE ICC, 2007.

[4] J.-M. Kelif, E. Altman, Downlink Fluid Model of CDMA Networks, in: Proc. of IEEE VTC Spring, 2005.

[5] J.-M. Kelif, M. Coupechoux, P. Godlewski, Spatial Outage Probability for Cellular Networks, in: Proc. of IEEE GLOBECOM, 2007.

[6] J.-M. Kelif, M. Coupechoux, P. Godlewski, Effect of Shadowing on Outage Probability in Fluid Cellular Networks, in: Proc. of WiOpt, 2008.

[7] G. Kulkarni, S. Adlakha, M. Srivastava, Subcarrier Allocation and Bit Loading Algorithms for OFDMA-Based Wireless Networks, IEEE Trans. on Mobile Computing 4 (6).

[8] G. Liu, J. Zhu, F. Jiang, B. Zhou, Y. Wang, P. Zhang, Initial Performance Evaluation on TD-SCDMA Long Term Evolution System, in: Proc. of IEEE VTC Spring, 2006.

[9] M. C. Necker, Coordinated Fractional Frequency Reuse, in: Proc. of ACM MSWiM, 2007.

[10] M. C. Necker, Local Interference Coordination in Cellular 802.16e Networks, in: Proc. of IEEE VTC Fall, 2007.

[11] T. D. Nguyen, P. Godlewski, Capacité OFDMA, Technical report, ENST (Télécom ParisTech) (2006).

[12] K. Ramadas, R. Jain, WiMAX System Evaluation Methodology, Tech. rep., WiMAX Forum (Jan. 2007).

[13] C. Tarhini, T. Chahed, On Capacity of OFDMA-based IEEE802.16 WiMAX Including Adaptive Modulation and Coding (AMC) and Inter-cell Interference, in: Proc. of IEEE Workshop on LANMAN, 2007.

[14] V. Erceg, L.J.Greenstein, et.al, An Empirically Based Path Loss Model for Wireless Channels in Suburban Environments, in: IEEE Journal on Selected Areas in Communications, 1999.

Fluid Model in OFDMA Networks

In this section, we recall the main results of the fluid model and derive the closed-form formula for SIR per subcarrier.

The key modeling step of the fluid model is replacing a given fixed finite number of BS by an equivalent continuum of transmitters which are spatially distributed in the network. This means that the transmitting power is now considered as a continuum field all over the network. In this context, the network is characterized by a user density ρ_u and a base station density ρ_{BS} [4]. We assume that users and BS are uniformly distributed in the network, so that ρ_u and ρ_{BS} are constant. We assume also that all base stations have the same output power per subcarrier P_{Tx}.

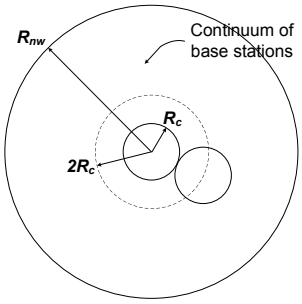

Fig. .1. Network and cell of interest in the fluid model; the distance between two BS is $2R_c$ and the network is made of a continuum of base stations.

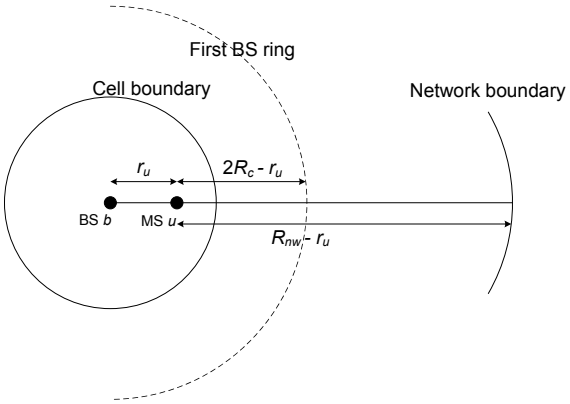

Fig. .2. Integration limits for interference computation.

We focus on a given cell, on a generic subcarrier and consider a round shaped network around this central cell with radius R_{nw}. The half distance between two base stations is R_c (see Fig..1 in case of reuse 1).

Let's consider a user u at a distance r_u from its serving base station b. Each elementary surface $zdzd\theta$ at a distance z from u contains $\rho_{BS}zdzd\theta$ base stations which contribute to $I_{ext,u}$. Their contribution to the external interference is thus $\rho_{BS}zdzd\theta P_{Tx}Az^{-\eta}$. We approximate the integration surface by a ring with center u, inner radius $2R_c - r_u$, and outer radius $R_{nw} - r_u$ (see Fig..2).

$$I_{ext,u} = \int_0^{2\pi} \int_{2R_c - r_u}^{R_{nw} - r_u} \rho_{BS} P_{Tx} A z^{-\eta} z dz d\theta$$

$$= \frac{2\pi\rho_{BS}P_{Tx}A}{\eta - 2} \left[(2R_c - r_u)^{2-\eta} - (R_{nw} - r_u)^{2-\eta} \right]. \quad (.1)$$

So, the SINR $\gamma_u \approx S_{b,u}/I_{ext,u} = P_{Tx}Ar_u^{-\eta}/I_{ext,u}$ can be expressed by:

$$\gamma_u = \frac{r_u^{-\eta}(\eta - 2)}{2\pi\rho_{BS}\left[(2R_c - r_u)^{2-\eta} - (R_{nw} - r_u)^{2-\eta}\right]}. \quad (.2)$$

Note that γ_u does not depend on the BS output power. This is due to the fact that we assumed an homogeneous network and so all base stations emit the same power on a given subcarrier. In this model, γ only depends on the distance r from the BS and can be defined in each location, so that we can write γ as a function of r, $\gamma(r)$. If the network is large, i.e., R_{nw} is big in front of R_c, γ_u can be further approximated by:

$$\gamma_u = \frac{r_u^{-\eta}(\eta - 2)}{2\pi\rho_{BS}(2R_c - r_u)^{2-\eta}}. \tag{.3}$$

The fluid model and the traditional hexagonal model are two simplifications of the reality. None is a priori better than the other but the latter is widely used, especially for dimensioning purposes. That is the reason why comparisons are performed throughout the paper.

Reference [5] has shown that the considered network size can be finite and can be chosen to characterize each specific local network's environment. This model thus allows us to do the analysis adapted to each zone while taking into account considered zone's specific parameters. Moreover, it can be noticed that the fluid model can be used even for great distances between the base stations.